



# Innovative approach for the protection of recycled concrete by biogenic silica biodeposition

Daniel Merino-Maldonado<sup>a,\*</sup>, Andrea Antolín-Rodríguez<sup>a</sup>, Lorena Serrano-González<sup>a</sup>, Saúl Blanco<sup>b</sup>, Andrés Juan-Valdés<sup>a</sup>, Julia M<sup>a</sup> Morán-del Pozo<sup>a</sup>, Julia García-González<sup>a</sup>

<sup>a</sup> INMATECO RESEARCH GROUP (Engineering of Materials and Eco-efficiency), Department of Agricultural Engineering and Sciences, University of León, Spain

<sup>b</sup> Department of Biodiversity and Environmental Management, University of León, Spain

## ARTICLE INFO

### Keywords:

Diatoms  
Surface treatment  
Biodeposition  
Biogenic silica  
Construction and demolition waste (CDW)  
Recycled concrete  
Durability

## ABSTRACT

Over the past few years, the construction industry has sought to be more sustainable through use of more economically responsible materials and the use of environmentally friendly techniques such as bio-remediation. One promising area in this regard is that of surface treatments, particularly bio-repair techniques, to reduce the deterioration suffered by cement-based materials as a result of environmental conditions. This study presents original work on the use of siliceous biodeposition by diatoms as a waterproofing surface treatment for recycled concrete. A recycled concrete mix containing a 50% substitution of recycled aggregates (RA) was used as a test substrate and the effectiveness of the bio-treatment was assessed using four different tests: capillary absorption, high-pressure water penetration, low-pressure water absorption and also characterised the biodeposited layer using SEM. Results demonstrate reductions of up to 33% in the capillary absorption test, while high-pressure water penetration decreased by 54.7%, compared to controls. In addition, Karsten tube tests showed low-pressure water absorption was delayed by up to 436 times relative to control samples. In combination these tests confirm the efficacy of diatom biodeposition as a protective surface treatment for cement-based construction materials.

## 1. Introduction

Uncontrolled population growth combined with the continued application of outdated linear economic models have contributed to the generation and accumulation of significant amounts of waste and low recycling rates. The construction industry has a significant role in all of this, finding it problematic to move away from these waste-producing linear models [1]. In recent years, however, numerous alternative models have been developed to manage construction and demolition waste (CDW), on a more sustainable, eco-friendly basis. Such approaches tend to involve the reuse of CDW, avoiding the over-exploitation of natural aggregates (NAs), and building a more circular economy overall [2]. The main goal of these innovations is to promote the recycling and reuse of materials while at the same time reducing waste generation, and is often associated with what is termed cradle to cradle design [3].

Concrete comprises up to 75 % NAs [4] and, the environmental

impact of its production is not only limited to consumption of NAs. Other considerations also include the generation of CO<sub>2</sub> emissions and the waste produced in its manufacture [5], all of which contribute to making the concrete industry a significant source of environmental pollution [6].

In this context, recent studies [7–10], have supported the use of recycled aggregates (RAs) in concrete manufacturing. Nevertheless, the use of RAs is limited, because these materials can reduce the mechanical properties and durability of concrete compared to that made conventionally [11]. This reduction in concrete quality arises because RAs are usually characterised by high porosity, high water absorption capacity, and low abrasion resistance [12] in comparison to NAs.

In this way, there is a direct relationship between the quality of concrete and the degree to which NAs are substituted by RAs with a substitution of less than 20 % being recommended according to international standards. However, with a focus on promoting the increased reuse of CDW in concrete manufacture, several studies exist to show

\* Corresponding author.

E-mail addresses: [dmerm@unileon.es](mailto:dmerm@unileon.es) (D. Merino-Maldonado), [aantr@unileon.es](mailto:aantr@unileon.es) (A. Antolín-Rodríguez), [lserg@unileon.es](mailto:lserg@unileon.es) (L. Serrano-González), [sblal@unileon.es](mailto:sblal@unileon.es) (S. Blanco), [andres.juan@unileon.es](mailto:andres.juan@unileon.es) (A. Juan-Valdés), [julia.moran@unileon.es](mailto:julia.moran@unileon.es) (J.M. Morán-del Pozo), [julia.garcia@unileon.es](mailto:julia.garcia@unileon.es) (J. García-González).

<https://doi.org/10.1016/j.conbuildmat.2023.130475>

Received 28 July 2022; Received in revised form 23 December 2022; Accepted 18 January 2023

Available online 26 January 2023

0950-0618/© 2023 The Author(s). Published by Elsevier Ltd. This is an open access article under the CC BY-NC license (<http://creativecommons.org/licenses/by-nc/4.0/>).

higher levels of substitution (greater than 50 %) are possible without significantly affecting the properties of the resulting concrete [13–15]. This research also seeks to foster sustainable approaches supporting a more circular economy, thus, this paper presents an examination how the properties of recycled concrete with a high percentage of substitution (50 %) can be improved by the use of a surface bio-treatment.

The use of biomaterials to protect surfaces has been common practice almost since human beings began building. In many parts of the world, for instance, there is a long history of using cactus extracts [16] and other natural products to waterproof facades and roofs. Nowadays, however, synthetic polymers are generally used instead of these biomaterials.

Although these new synthetic polymers have similar or even greater effectiveness than the biomaterials they replaced, their use is now being questioned. This is because these products have major environmental drawbacks, such as their non-biodegradability and other harmful effects on the ecosystem [17]. New alternatives are urgently needed and biological protective agents such as diatoms are among the contenders.

Diatoms are unicellular, photosynthetic microorganisms which play a key role in several of the biosphere's geochemical cycles. Diatom cells have siliceous exoskeletons called frustules which are formed almost entirely of hydrated silica ( $\text{SiO}_2$ ). These frustules are very intricately patterned, with each one consisting of two valves held together by girdle bands (also made of silica). In turn, each valve comprises a set of stacked hexagonal chambers separated by silica plates. There are almost  $10^5$  different known diatom species and all feature unique frustule architectures many of which can teach us valuable lessons concerning mechanical properties as well as the construction of advanced materials with many different practical applications [18]. Diatoms are the principal organism involved in the biosilicification process; indeed, not only do they produce the greatest variety of silicified structures, but they are also the largest producers of biogenic silica [19].

Many diatom species are able to interact with and adhere to submerged surfaces, including human-made underwater structures, forming coatings called biofilms. For this reason, understanding and improving the interactions between underwater infrastructures and biological components remains one of the ecological engineering challenges [20]. Hence, several papers on the subject [21–23] have focused on understanding the processes involved in initial biofilm development, the morphology and biochemistry of adhesion structures, the mechanical properties of adhesives and the study of the adhesion strength of whole cells to surfaces of different chemical compositions.

In general, it appears to be the diatoms that initiate surface colonization and biofilm formation, although the exact mechanisms involved are not fully understood [24]. What has been determined are that biofilm formation includes several distinct phases. The first of these phases is the development of a primary coating formed of colloidal organic matter, polysaccharides, and proteins. This is immediately followed by the accumulation of microorganisms (bacteria, diatoms, fungi, and microalgae) which secrete EPS (Extracellular Polymeric Substances) during attachment, promoting further colonization and population growth [21]. On contact and adhesion to a given surface, diatoms migrate to those areas that provide them with the best environmental conditions [22], for instance, to surface crevices and niches that can provide protection from hydrodynamic shear forces that would otherwise limit diatom adhesion and growth rates. Thus, diatom distribution throughout the biofilm is heterogeneous, with micro-scale variations [21] dependant on surface roughness and microtopography [23]. In addition, physical, chemical and biological changes in the environment also affect diatom communities causing temporal fluctuations in population numbers and distribution [21]. To date, research into protective bio-treatments for concrete has considered the use of bacterial calcium carbonate biodeposition [25–28] or the direct application of laboratory-synthesised nano-silica [29–32].

Diatoms have received some attention as a self-cleaning bio-coating for glass, ceramics, or glass-ceramics [33], however, the huge potential

for these organisms as a protective treatment for concrete has so far not been explored. The present paper seeks to address this gap in the literature and thus focuses on characterising the properties of biodeposited diatom frustules as a surface coating for concrete. It is proposed that such a coating could be a practical way to seal and repair concrete extending its lifetime and preventing the overexploitation of raw materials in the construction industry.

## 2. Materials and methods

### 2.1. Materials

#### 2.1.1. Concrete

The concrete used in this study was composed of a mix containing blast furnace slag cement CEM Type III/A 42.5 N/SR (compliant with all chemical, physical and mechanical requirements stipulated in EN 197-1:2011 [34]); coarse aggregates including both recycled and natural aggregates; and fine aggregate in the form of natural siliceous sand. Water was added to this mix in a water-cement ratio of 0.59 to obtain concrete with a plastic consistency. The exact quantities of the materials used in this concrete mix are shown in Table 1.

The coarse aggregates used in this study were supplied by the CDW management company, Valdearcos S.L., located in the province of León (Spain). The specific mix comprised a 50:50 ratio of natural (siliceous river gravel) and recycled aggregates (concrete waste).

The aggregates were characterised in terms of particle density and water absorption ( $\text{WA}_{24}$ ) using the standard tests recommended in EN 933-1:2012 [35] and EN 1097-6:2014 [36]. Table 2 shows the differences between the properties of fine aggregates (natural siliceous sand, particle size 0–4 mm) and coarse aggregates (NAs: river siliceous gravel, particle size 4–12.5 mm; and RAs: waste concrete, particle size 4–12.5 mm).

It should be noted that all the aggregates used in this study met the requirements of the Spanish Structural Code [37] and European standard EN 12620:2003 + A1 [38].

RAs generally have a high water absorption [39] thus, due to the high percentage of these aggregates in this mix, it was necessary to assess the particular characteristics of these aggregates. This was done using the standard test outlined in EN 933-11:2009 [40], see Table 3.

Once the concrete was mixed, specimens were placed in steel moulds and cured for 28 days at  $20 \pm 2$  °C with 100 % relative humidity. There were four different mould geometries, one designed for each of the tests to be completed (three for durability tests and one for SEM).

In addition, compressive strength was determined in the hardened state as per EN 12390-3:2020 [41] of cylindrical specimens ( $200 \times 100$  mm) of the samples after treatment (35.4 MPa) and without treatment (33.9 MPa).

#### 2.1.2. Diatoms

In this work, diatom biodeposition is used as a biological surface treatment for concrete. This biodeposition in the form of biogenic silica [19] involves the adhesion of diatom frustules to the surface of the concrete to form a coating known as a biofilm. These biofilms are generally dominated by motile diatoms and their secretions, specifically adhesive mucilages made by extracellular polymeric substances or EPS [22].

**Table 1**  
Recycled concrete composition.

Material	Composition ( $\text{kg}/\text{m}^3$ )
NA	585.5
RA	585.5
Sand	642
Cement	354
Water	210

**Table 2**  
Aggregate characterization.

Aggregate	Fraction (mm)	D/d Ratio	Density $\rho_p$ (Mg/m <sup>3</sup> )	WA <sub>24</sub> %
NA	4–12.5	2.66	2.63	4.3
RA	4–12.5	3.33	2.54	4.8
Sand	0–4	6.65	2.55	1.7

**Table 3**  
Composition of recycled aggregates.

Parameter	Value
Composition	(%)
Rc (concrete)	47.2
Ru (natural Stone)	51.6
Rb (bricks and tiles)	0.2
Ra (bituminous material)	0
Rg (glass)	0
Fl (floating particles)	0
X (gypsum and impurities)	1

In order to develop the biofilms for this investigation, specimen concrete samples were submerged in a pond. The particular tests to be completed required the preparation of 4 different types of specimen in terms of surface area and shape. After the period of biofilm growth, specimens were removed and prepared for testing. Three of the specimens prepared in terms of chlorophyll concentration and the diatom guilds and families present were characterised (Table 4).

To quantify the diatoms in the biofilms formed, the average chlorophyll concentration ( $\mu\text{g Chla}/\text{mm}^2$ ) of the specimens per unit area was measured (Table 4). This value ( $2,64 \times 10^{-5} \mu\text{g Chla}/\text{mm}^2$ ) allowed us to calculate the absolute amount of chlorophyll on each of the treated test surfaces.

The species present in a given diatom community can be categorised into what are termed guilds. Environmental factors influence the growth of different diatom guilds; thus, samples were distributed across the pond to experience a range of environmental conditions to test the potential variability of the diatom populations used in this study. Fig. 1 shows the percentages of several common diatom guilds present in the biofilm. Although a huge variety of other species were present, three groups in particular stood out: the Epontic (planktonic), Bentic (benthonic guilds), and Epontic & Bentic (both life forms) species. Results for each of specimen types are shown on Fig. 1.

In terms of family characterisation, the classification focused on six predominant families. Analysis showed that the majority of diatoms in the biofilms belonged to the Naviculaceae and Monoraphids family. Other families present, in decreasing order of abundance, were the Araphids, Epithemiaceae, and Surirellaceae (Fig. 2).

**Table 4**  
Concentration of diatom biodeposition.

Parameter	Average	Specimen type I 400*100*100 mm	Specimen type II $\varnothing$ 150*300 mm	Specimen type III 100*100*100 mm
Concentration ( $\mu\text{g Chla}/\text{mm}^2$ )	$2.64 \times 10^{-5}$			
Test Surface ( $\text{mm}^2$ )		400*100	$\pi*75^2$	100*100
$\mu\text{g Chla}$ per specimen		1.056	0.466	0.264

## 2.2. Methods

### 2.2.1. Concrete surface treatment

Three different tests were developed to assess the water-resistant properties of biofilms deposited on concrete. Each test required the preparation of concrete samples with particular properties in terms of surface area and cross-section, thus three specimen types were classified according to these two properties, see Table 5. Concrete was mixed and poured into specially designed moulds to create the required geometries. Efforts were made to ensure the test face of each specimen (the biofilm substrate) was as flat as possible. The concrete was cured for a period of 28 days after which, the specimens were immersed in a pond for 3 months exposed to environmental factors and without addition of specific nutrients during diatom growth since it was previously verified that the growth of the diatoms was adequate. The immersion area is located in León (Spain) in the grounds of the Environmental Institute of the University of León, with an altitude of 824 m above sea level and co-ordinates of  $42^{\circ}36'16''\text{N}$ ;  $5^{\circ}33'26''\text{W}$ .

The specimens of each test type were randomly distributed over the surface of the pond to analyse diatom guilds and immersed to a depth of  $20 \pm 5$  cm below the water surface, with the specimen's test face parallel to the water surface. In this way, spontaneous microalgae growth was encouraged on the uppermost concrete surface.

According to Admiraal et al. [42], environmental factors such as temperature and daylight hours are limiting factors in diatom growth. In this way, diatom growth is optimal when the photoperiod is positive, that is, when the number of hours of daylight is increasing exponentially [43]. This period coincides with the spring equinox in the northern hemisphere; thus, specimens were immersed in water for a period of 3 months from March to June. Climatological data was collected for this period including solar radiation levels and temperatures (Fig. 3). It was calculated that, over this period, the developing biofilms were exposed to a total of 1044 h of sunshine.

According to Lacoursière et al. [43] mature diatom colonies can be established on an artificial substrate in as little as 4 weeks, however, the density of those biofilms was low. Thus, a minimum 3-months growth period was established for the biofilms produced in this study to ensure they contained sufficiently high numbers of individual diatoms and levels of silica biodeposition, physically attached to the concrete surface.

After the biofilm growth period, specimens were removed from the pond and left to dry in the laboratory at a temperature of  $20 \pm 2$  °C and a humidity of  $50 \% \pm 10 \%$ , for 7 days.

For the purposes of comparison, a set of control specimens (untreated concrete moulds) was prepared. After curing, these specimens were immersed in covered water tanks without light, to prevent the growth of any biological material. This immersion period lasted for three months after which point specimens were removed from the water and dried under the same conditions as the biofilm-treated samples.

### 2.2.2. Measurement of biogenic silica SEM and EDX analysis

Following the standard Spanish protocols for the collection of benthic diatoms EN 13946:2014 [44], adapted for use in lentic systems, *Periphyton* samples were collected from the experimental substrates. In brief, epilithon was collected from various sites in the experimental pond bed using a brush to gather a sample from a known surface area. Sampling surfaces were selected to meet certain criteria of which the most important were: being within the photic zone; sufficiently deep and stable; clear of sediment and macroalgae. Samples were placed together in a single 50 mL vial and preserved in formaldehyde (4 % v/v) until required.

For analysis, a clean suspension of diatom frustules was needed. To achieve this, the preserved samples were first treated to remove all organic matter by the addition of hydrogen peroxide (120 vols.) at 90 °C for 3 h. Samples were then centrifuged and decanted several times. The resulting suspension was then mounted on slides using a high refractive index synthetic resin ready for examination under the microscope.

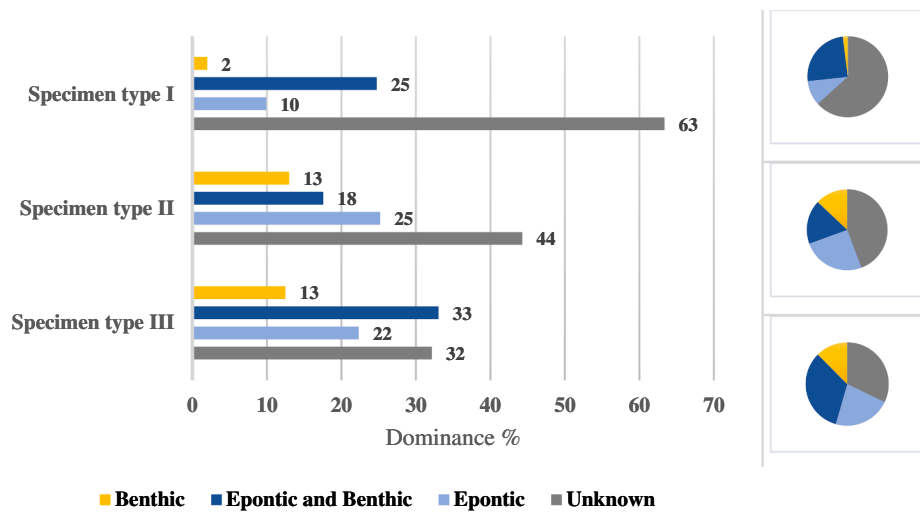


Fig. 1. Distribution of the different diatom guilds by specimen type.

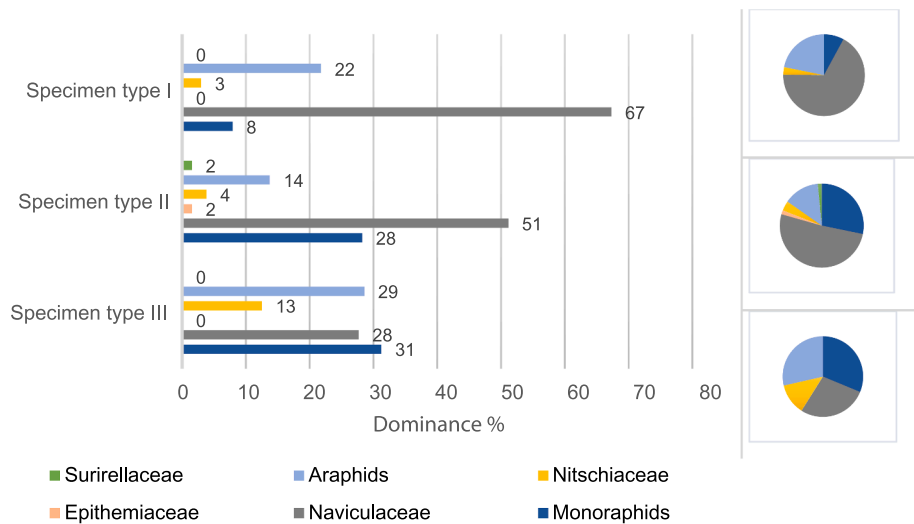


Fig. 2. Distribution of the different families of diatoms by specimen type.

Table 5  
Types of samples by tests.

Test methods	N°	Dimensions (mm)	Test Surface (mm <sup>2</sup> )
Karsten Tubes-Type I	4	400*100*100	400*100
Water Under Pressure -Type II	6	Ø 150*300	$\pi*75^2$
Capillary Water Absorption -Type III	6	100*100*100	100*100
SEM	6	Ø 25*10	$\pi*1,25^2$

The slides were analysed at 1000× magnification using a brightfield photomicroscope with phase contrast condenser. To count and identify diatoms, the standard protocols contained in EN 14407:2015 [45] were followed. A minimum of 400 individuals were quantified and identified to the lowest possible taxonomic level, following Hofmann et al. [46] and the references contained therein. Numerical results were processed with OMNIDIA v. 4.2 [47] to obtain the trophic diatom indices for each sample. The result of each method is a numerical value that expresses the profile and ecological preferences of each taxon according to the classification into life forms published by different authors.

In addition, whole biofilm production was evaluated using chlorophyll *a* concentration as a proxy. Thus, chlorophyll *a* was extracted from

filtered GF/F samples in 90 % ethanol and determined spectrophotometrically according to ISO 10260:1992 [48].

For the SEM imaging of the biofilms produced for this study, samples cured concrete were cut to the correct dimensions (diameter = 25 mm and height = 10 mm, see Table 5) by placing a drop of the sample on a conductive metal structure on a conductive adhesive and allowing it to dry at room temperature. The samples were then coated with a 10 nm thick carbon layer using a high vacuum modular metallisation system (QUORUM Q150T ES). The study was performed with a MERLIN microscope (Carl Zeiss), operating at 20 kV.

### 2.2.3. Durability testing

The particular focus of this work is to assess the effectiveness of diatom biofilms in increasing the water resistance of concrete. To this end, concrete substrates with diatom biofilms were compared to untreated concrete substrates in a variety of tests of surface porosity and water absorption. The tests are described below.

2.2.3.1. Determination of capillary water absorption of hardened concrete. The capillary water absorption coefficient of a material is a measure of its water absorption capability and its porosity. It can be found experimentally by placing one surface of a material in contact

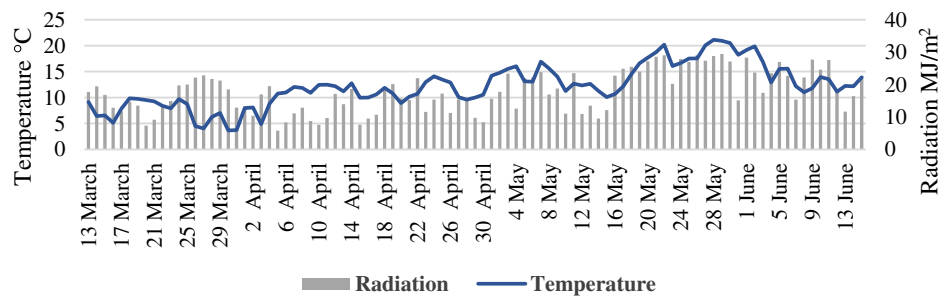


Fig. 3. Environmental Factors.

with water and taking consecutive measurements of the material's weight as it absorbs the liquid.

This test was completed using the cubic  $100 \times 100 \times 100$  mm specimens (Table 5). Three control sample (C-sample) and three diatom sample (D-sample) were tested and compared. To ensure that absorption only occurred at the test surface, the lateral faces of the concrete blocks were waterproofed with a 1 cm thick paraffin layer.

The specimens were conditioned according to standard EN 83966:2008 [49] and the standard EN 83982:2008 [50] capillary absorption test was used. The temperature and humidity were kept constant at, respectively  $20 \pm 2$  °C and  $55 \% \pm 10$  % (note that the humidity was not permitted to fall below 45 % during the test, as stipulated by the standards used).

Specimens were placed in a lidded plastic container containing a 5 mm depth of water. Specimens were positioned on a plastic grille so that they remained level and in contact with the water.

All specimens were weighed after conditioning and just before contact with the water. Once in contact with the water, specimens were then weighed at intervals of 5 min, 10 min, 15 min, 15 min, 15 min, 30 min, 1 h, 2 h, 3 h, 4 h, 6 h, 24 h, 48 h, 72 h, 96 h, 120 h until they reached a constant mass (assessed as the point at which the difference in mass between two consecutive weighing times was smaller than 0.1 %), being registered the cumulative water absorption of the specimens.

Plot of cumulative water absorption against the square root of the test duration time allowed to calculate the capillary water absorption coefficient  $K$  for the specimens (EN 83982:2008 [50]), according to Eq. (1).

The value of  $K$  is related to other properties of concrete, such as the effective porosity of the concrete  $\epsilon_e$ , and resistance to water penetration by capillary absorption,  $m$ , in the following way:

$$K = \frac{\delta_a \cdot \epsilon_e}{10 \cdot \sqrt{m}} \quad (1)$$

**2.2.3.2. Depth of water penetration under pressure.** The depth of water penetration under pressure for hardened concrete was assessed according to the standard test, EN 12390-8: 2020 [51]. In this test the  $\varnothing 150 \times 300$  mm cylindrical specimens (Table 5) were used and, as in the previous test, three C-sample and three D-sample specimens were tested and compared. A water penetration rig (product number 270200: Mecánica Científica S.A, Madrid, España) comprising three compressed air driven hydrostatic pressure stations. These provided water at a pressure of 5 bar (0,5 MPa), and this was applied to the concrete samples over a period of  $72 \pm 2$  h.

After the 72-h period of exposure to high-pressure water, specimens were subjected to indirect tensile stress to produce a fracture perpendicular to the test surface. In this way the depth of water penetration could be observed. This procedure was completed in accordance with EN 12390-6:2010 [52].

For the analysis of the water penetration front, the maximum penetration depth " $P_{max}$ " and the average penetration depth " $P_m$ " were calculated according to EN 12390-8:2020 [51]. The water penetration front was analysed using ImageJ software [53] enabling the calculation

of  $A_{pf}$  ( $mm^2$ ), the area of the penetration front. Using the value of  $A_{pf}$ , the average penetration depth  $P_m$  could be calculated according to Eq. (2):

$$P_m = \frac{A_{pf}}{d} \quad (2)$$

Where  $d$  is the specimen's diameter (mm).

**2.2.3.3. Water absorption at low pressures.** Low-pressure water absorption was tested using the Karsten tube method. The water pressures used here simulate the effects of rainfall on the concrete surface allowing the assessment of the effects of particular surface treatments [54] under conditions that approach those of real-life, everyday usage.

The testing protocol used is contained in EN 16302:2016 [55]. The test uses so-called Karsten tubes, specially shaped glass tubes, graduated to tenth of a millimetre, which are adhered to the test surface using butyl adhesive. The  $400 \times 100 \times 100$  mm specimens were used for this test (Table 5) and the Karsten tubes were distributed homogeneously across the test surface using a minimum separation of 40 mm between tubes to avoid interactions between them. As before C-sample and D-sample specimens were tested and compared, in this case however there were two of each sample type, with 6 points of data collection per specimen.

Once the Karsten tubes were in place each tube was filled to the zero marker with distilled water. Then, the time taken for the water level to drop 1 mL, meaning for the concrete to absorb 1 mL of water, was measured.

### 3. Results and discussion

#### 3.1. Determination of capillary water absorption of hardened concrete

The results obtained in the capillary water absorption test are shown in Fig. 4 where the change in weight of the concrete due to water absorption (cumulative water absorption) is plotted as a function of  $t^{1/2}$ . The curve demonstrates two phases of water absorption: an initial rapid phase dominated by the capillary force during which the finest pores in the material are filled and a second phase where the water front has reached the top surface of the specimen and further absorption is determined by the rate at which trapped air can diffuse out of remaining pores in the concrete [56,57].

The results showed that C-samples continued to absorb water for a longer period of time compared to D-samples: C-samples reached a constant mass at 120 h ( $85 \text{ min}^{0.5}$ ), while the mass of D-samples stabilised between 72 ( $66 \text{ min}^{0.5}$ ) and 96 ( $76 \text{ min}^{0.5}$ ) hours (Fig. 4). In addition, C-samples absorbed a higher total amount of water than D-samples. From Fig. 4, it can be seen that biodeposition appears to reduce the capillary water absorption capacity of concrete by 29 % compared to untreated concrete.

Calculations of the water absorption coefficient,  $K$ , provided further evidence of the effectiveness of diatom biodeposition in reducing the water permeability of concrete. As can be seen on Fig. 5, both samples had  $K$  values smaller than the maximum permitted value ( $1.29 \times 10^{-2}$

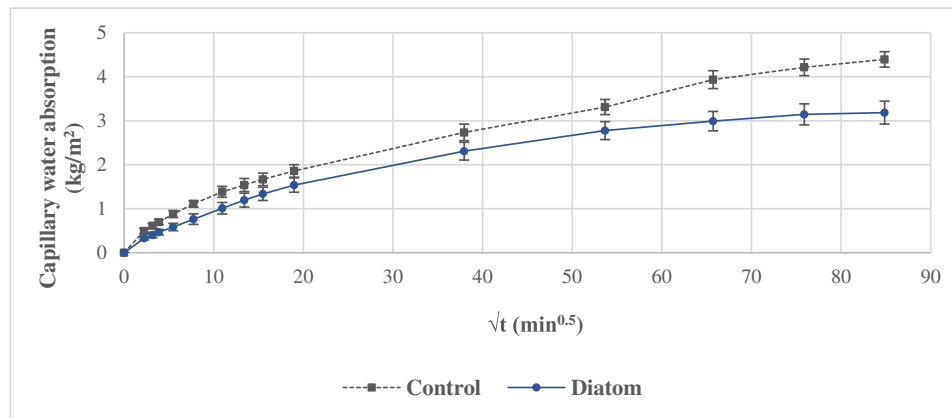


Fig. 4. Curve of capillary water absorption in hardened concrete samples.

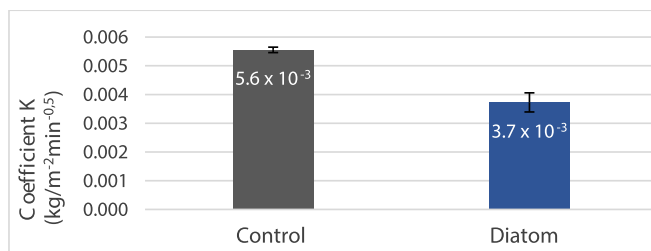


Fig. 5. Capillary absorption coefficient “K”.

( $\text{kg m}^{-2} \text{min}^{-0.5}$ ), defined in standard EN 1504-2:2005 [58]), with the diatom treated concrete having the lowest value. Referring to Fig. 5, the low K value shown by D-samples suggests a more than 33 % improvement in water resistance compared to C-samples. This demonstrates that diatomaceous silica biodeposition effectively seals the pores in the concrete thus lowering capillary water absorption.

Capillary absorption is the main form of liquid transport in cementitious materials due to their porous nature [59]. This presents a problem in the use of these materials for construction as it is not just water that may be transported but also corrosive materials and these may damage the integrity of the concrete [60].

These results compare favourably with other studies into waterproofing treatments for concrete. For example, Geng et al. [30] treated concrete with combinations of 50.5 % silane emulsion and a Nano-SiO<sub>2</sub> preparation made using the sol-gel process. The silane emulsion (600 g/m<sup>2</sup>) alone was found to reduce the water absorption coefficient of concrete by 70 %. However, the most effective treatments were those based on Nano-SiO<sub>2</sub> (300 g/m<sup>2</sup>)/silane emulsion (300 g/m<sup>2</sup>) layers, which reduced the water absorption amount by more than 75 % compared to the control. In a similar study, Shirzadi Javid et al. [61] used Nano-SiO<sub>2</sub> mixed with deionised water and achieved significant decreases in the water absorption coefficient (40 %) at lower nano-particle concentrations (20 %).

More in line with the research presented in this study, De Muynck et al. [25], investigated the biodeposition of carbonates produced by *B. Sphaericus* LMG bacteria (10<sup>7</sup> cells/mL). The bacteria caused improvements to water resistance of 47 % which was compared to a silica-based treatment, silane that gave a 79 % improvement. In another study, Yazdi et al. [28] used a combined treatment involving bacterial CaCO<sub>3</sub> and a nano-silica treatment and found that the treatment significantly improved the water resistance and thus the overall durability of their samples.

### 3.2. Depth of water penetration under pressure

Fig. 6 a shows the maximum water penetration depth,  $P_{\text{max}}$  (mm), observed for C-samples and D-samples. The Spanish structural code for concrete [37], establishes a upper limit of  $P_{\text{max}} = 30$  mm for concrete to guarantee its durability. The value of  $P_{\text{max}} = 18$  mm obtained for C-samples indicates that the recycled concrete used in this investigation is already sufficiently water resistant to meet current standards and performs significantly better than other experimental mixes with similar percentages of waste concrete RAs, for example, Matar and Barhoun [62] recorded  $P_{\text{max}} = 39$  mm while results from a study by Quedou et al. [63] gave this value as 25 mm. Furthermore, the value of  $P_{\text{max}}$  found for D-samples was 25.4 % lower than that for C-samples.

Looking at results for the average water penetration depth,  $P_m$  (mm), here the difference in performance between untreated and diatom treated concrete are even more significant. In fact, the value of  $P_m$  for D-samples is 54.7 % lower than for C-samples (Fig. 6b). The difference between maximum and average penetration depth is significant because biodeposition does not necessarily result in a coating of constant thickness. Variations in the distribution of diatom frustules across the test surface mean that the maximum penetration depth can be much greater than average penetration depth, thus, the latter is a more representative measure of the effectiveness of the biodeposited coating.

Considering Fig. 7, it can be appreciated that water penetration in C-samples is homogeneous whereas in D-samples there are areas where no water has penetrated at all. Further investigation into the composition of the biodeposited coating revealed that while the concentration of diatoms was quite constant across the test surface, the range of species found in the permeable and non-permeable areas was different. Biodeposition is a natural process and will be affected by local environmental conditions, thus, the variation in species distribution is unsurprising and has been reported in other work [26]. However, it is interesting to examine which diatom species appear to offer the best water-resistant properties. Fig. 8, shows the results of a component analysis completed on the diatom populations found either at the permeable or the non-permeable regions of test surfaces and demonstrates the existence of differences at the community level. The taxa occurring in the permeable zones (grey polygon) are mainly planktonic genera such as *Fragilaria* (FRAG) or *Tabellaria* (TABE), whose presence on the test surfaces may be due to passive sedimentation from water column. The non-permeable zones (red polygon), on the other hand, were typically characterised by epilithic species such as *Eolimna minima* (EOMI), *Achnanthyidium pyrenaicum* (ADPY) or *Navicula cryptotenelloides* (NCTO), which form a true algae biofilm on the concrete substrate.

This test is considered one of the most important for determining the permeability of hardened concrete. The high porosity of concrete means that water can penetrate deep into the material so decreasing its durability [64], thus low water permeability is a desirable quality in

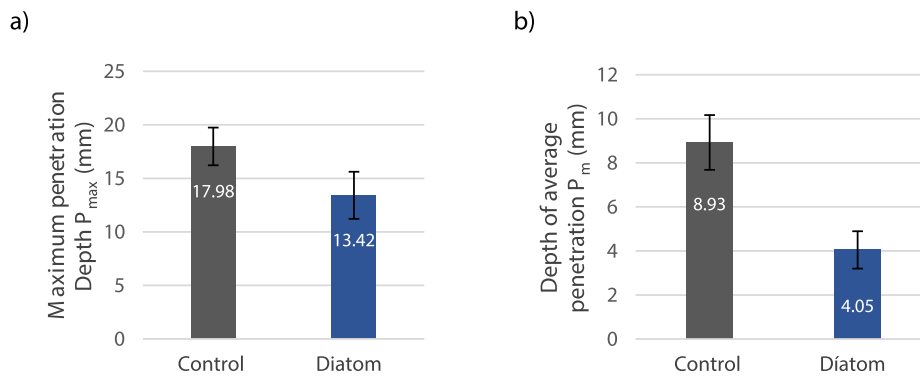


Fig. 6. Result of water penetration under pressure: a) Maximum penetration Depth  $P_{max}$ ; b) Depth of Average Penetration  $P_m$ .

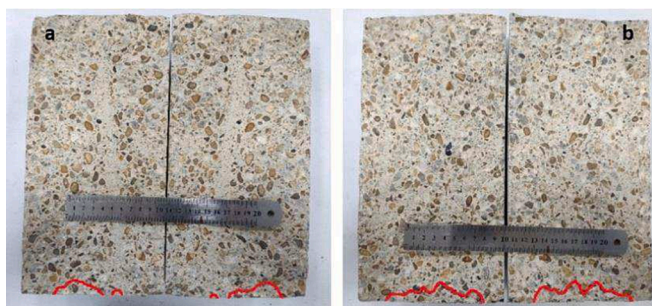


Fig. 7. High pressure water penetration front: (a) Diatom sample; (b) Control sample.

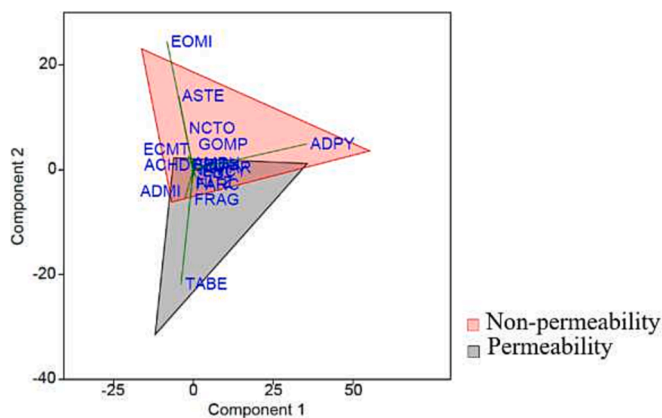


Fig. 8. Principal component analysis of the type of species found in permeable and non-permeable areas.

concrete.

Relevant studied in the area of water-proofing bio-treatments includes that of Xu et al. [27], this work compared  $CaCO_3$  biodeposited coatings made by *S. Pasteurii* DSM 33 bacteria cultures ( $3 \times 10^8$  cells/mL), in either a liquid or semi-solid medium. Their results indicated that these biological coatings could increase concrete resistance to water penetration by 45 % for bacteria in the liquid medium and 57 % for bacteria in the semi-solid medium. Creating an effect similar to that of silica frustules, Ardalan et al. [29] managed to improve the permeability of concrete by spraying it with colloidal nano-silica at concentrations of up to 12 %. They obtained reductions in the water penetration front of 31 % with respect to control samples, corroborating other results reported by, for instance, Shirzadi Javid et al. [61], who used a 40 % concentration nano-silica spray and obtained a 48 % decrease in water penetration depth compared to reference samples.

### 3.3. Water absorption at low pressures

Fig. 9 shows the results obtained for C- and D-samples in the low-pressure (Karsten tube) water absorption test. The graph shows the amount of water was absorbed by the concrete as a function of time and gives the overall time it took for 1 mL of water to be absorbed. Comparing the C-samples and D-samples, it is possible to see that the time taken for D-samples to absorb 1 mL of water was significantly (436 times) greater than for C-samples. In addition, Karsten tubes distributed across each test surface gave similar results showing that test surfaces were uniform.

Referring to Fig. 9, it is interesting to note that both the initial rate (up to 0.2 mL) of water absorption for both control and diatom samples is similar. The curves for the two samples then diverge with the rate of absorption for C-samples increasingly higher than that for D-samples which causes the absorption times of the D samples to increase. These results demonstrate that diatomaceous silica is an effective water-proofing treatment for concrete creating a similar hydrophobicity as observed for nano-Silica coatings [31].

Low-pressure water testing has been used in several other studies to assess the waterproofing abilities of several treatments. Liu et al. [65] investigated the effectiveness of bacterial  $CaCO_3$  biodeposition produced by *Bacillus Pasteurii* bacteria inoculum (DSM 33) as a water-resistant coating. They achieved up to 90 % improvement in water resistance compared to untreated concrete when using the highest bacterial cell concentrations ( $1 \times 10^9$  cells/mL). Other work has used silicon-based materials, as in the presented study, for instance, Sakr et al. [32] treated samples with a coating made from colloidal nano-silica (50 % concentration) and a mix of silane and montmorillonite nano-clays (90 meq/100 concentration). Their results showed that treated samples demonstrated absorption times 78–90 % greater than untreated samples showing clear evidence that nano-silica is able to reduce the porosity of concrete creating a hydrophobic protective layer.

### 3.4. SEM and EDX analysis

Fig. 10 shows SEM micrographs and EDX spectra of a typical D-sample (a) and a typical C-sample (b). The siliceous nature of the bio-coating on D-samples is confirmed by the EDX spectrum for this sample which shows strong peaks for Silicon and Oxygen demonstrating that  $SiO_2$  is the dominant component of the film.

Referring to the micrographs, Fig. 10 a shows, the structure of the silica biofilm deposited on the concrete samples. As expected, of the density of diatoms adhering to the surface is not uniform across the sample, indeed there appears to be new diatom accumulation over older deposits producing overlapping layers as seen in the research by Georges et al. [20] using a mortar substrate. The Benthic diatom species observed in Fig. 10a, can be seen to accumulate together, forming large mats of fused and overlapping adhesive material in a process known as rafting [22]. As discussed by Chiovitti et al. [66] diatoms achieve permanent

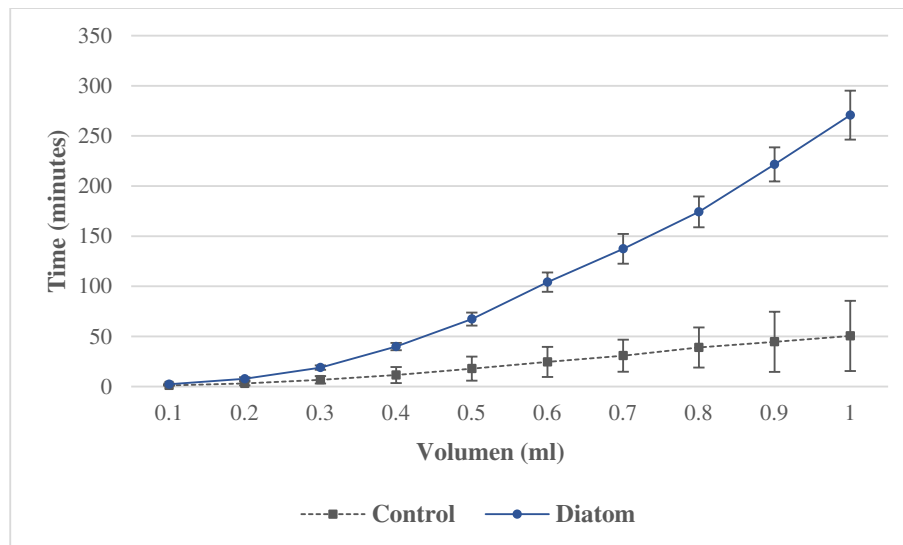


Fig. 9. Result of Karsten tube water absorption test.

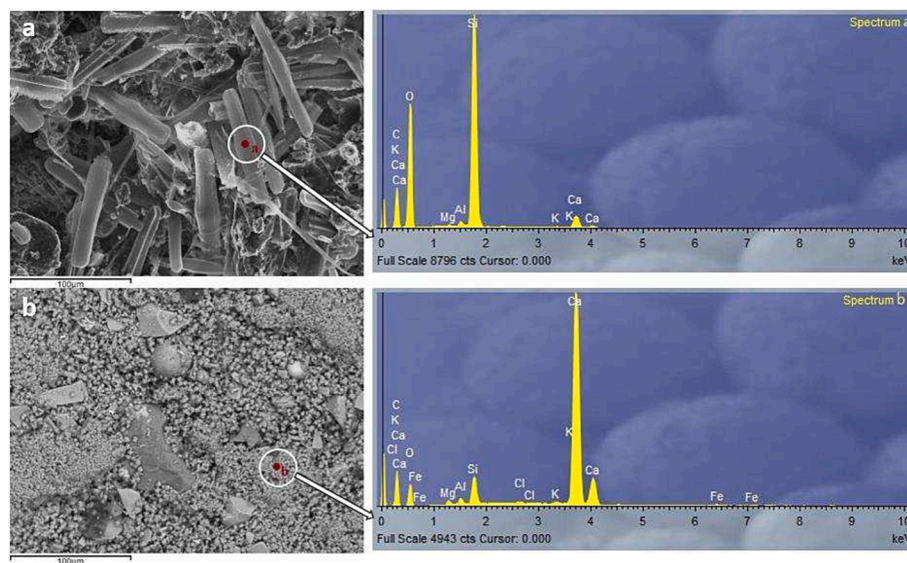


Fig. 10. SEM images showing surface microstructures and EDX spectra to show elemental compositions: (a) Diatom sample; (b) Control sample.

adhesion to surfaces such as concrete by depositing a mucilaginous material comprising a complex, as yet largely undefined mixture of proteins, proteoglycans and carbohydrates. This material forms pad- or stem-like structures that anchor the diatom to the substrate.

Comparing Fig. 10a and b, while the pores in the concrete substrate are clearly visible on the surface of the C-sample, on the bio-treated D-sample, however, these are entirely covered and protected. As discussed by Ardalan et al. [29], SiO<sub>2</sub> protective coating such as the one studied in this research interact with the microstructure of the concrete surface to decrease the interconnectivity between surface pores and the micrographs seen in this study, showing diatom frustules filling the concrete substrate surface pores, tend to support this. The pore-filling capability of diatom frustules is almost certainly the explanation for the improvements in water resistance observed in these results.

#### 4. Conclusions

This study investigated the effectiveness of a biological treatment to improve the water-resistance of recycled concrete. The bioproduct used

in this work was based on the biodeposition of diatom frustules and the treatment was applied to concrete samples made from a mix containing 50 % recycled concrete aggregates. Concrete samples treated with diatom biodeposited silica were subjected to several tests of water permeability and the performance of the film was assessed with respect to untreated control samples. Furthermore, it was demonstrated that there was no biodeterioration of the mechanical properties after treatment, with hardly any significant differences in the compressive strength test.

In tests of capillary absorption, concrete treated with diatom biodeposition showed a 33 % lower capillary water absorption compared to untreated controls. Treated samples also reached a steady state (gained no more mass) up to 48 h earlier than control samples. From this it can be concluded that the diatom biodeposition acts on the large-scale pore network and decreases the water absorption in concrete.

Some particularly interesting results were obtained for high-pressure water absorption tests, most important of which was that the biofilm reduced the average depth of water penetration ( $P_m$ ) by up to 54.7 % compared to control samples. The maximum penetration depth was also



reduced for bio-treated concrete, but it was noted that, whereas water penetration of control samples was homogenous, in bio-treated samples was quite uneven. This is because, biodeposition treatment is heterogeneous across the substrate surface: due to environmental factors the density and types of species adhering to the concrete will vary.

Low water pressure tests (Karsten tubes) also showed the diatom biodeposited film had significant water-proofing effects. In these tests, the treated surfaces behaved uniformly and showed that the biofilm reduced water absorption by up to 436 %.

In conclusion, the results presented demonstrate the effectiveness of diatom biodeposited silica as a waterproofing surface treatment for concrete: bio-treated samples showed lower water absorption and lower levels of water permeability than untreated control samples. The use of a treatment such as that investigated could help promote a circular economy in the construction industry as it would significantly improve the durability of recycled concrete, increasing its useful life and thus reducing the industry's use of raw materials.

Furthermore, the effectiveness of the treatment investigated compares well with other alternatives currently being studied in terms of performance and, as a biological agent, it is both more environmentally friendly than the petrochemical-based treatments currently in use. At present, despite its advantages, there is very little research into the topic of biologically derived silica as a surface treatment for concrete. Based on the very promising results presented in this work, it would suggest that this area needs further research.

#### CRediT authorship contribution statement

**Daniel Merino-Maldonado:** Data curation, Formal analysis, Investigation, Methodology, Software, Writing – original draft, Writing – review & editing. **Andrea Antolín-Rodríguez:** Investigation, Methodology, Data curation. **Lorena Serrano-González:** Investigation, Methodology, Data curation. **Saúl Blanco:** Investigation, Methodology, Data curation, Conceptualization, Supervision. **Andrés Juan-Valdés:** Conceptualization, Supervision, Writing – original draft, Writing – review & editing. **Julia M<sup>a</sup> Morán-del Pozo:** Formal analysis, Resources, Writing – review & editing. **Julia García-González:** Formal analysis, Supervision, Writing – original draft, Writing – review & editing.

#### Declaration of Competing Interest

The authors declare that they have no known competing financial interests or personal relationships that could have appeared to influence the work reported in this paper.

#### Data availability

Data will be made available on request.

#### Acknowledgements

The authors are grateful for the PhD fellowships from the Regional Government of Junta de Castilla y León published in the ORDER EDU/601/2020 and the ORDER EDU/875/2021, co-financed by the European Social Fund. SEM images were kindly provided by A. Olenici at the Electronic Microscopy Unit of the University of Jaén (Spain). Technical and human support provided by CICT of Universidad de Jaén (UJA), MINECO, Junta de Andalucía, FEDER) is gratefully acknowledged.

#### References

- [1] A. Nadazdi, Z. Naunovic, N. Ivanisevic, Circular economy in construction and demolition waste management in the Western Balkans: A sustainability assessment framework, *Sustain.* 14 (2022) 871, <https://doi.org/10.3390/su14020871>.
- [2] E. Commission, Communication from the Commission to the European Parliament, the Council, the European Economic and Social Committee and the Committee of the Regions: A new action plan for the circular economy towards a cleaner and more competitive Europe, Brussels, Belgium, 2020. <https://www.un.org/sustainabledevelopment/sustainable-consumption-production/>.
- [3] P. Ghisellini, M. Ripa, S. Ulgiati, Exploring environmental and economic costs and benefits of a circular economy approach to the construction and demolition sector. A literature review, *J. Clean. Prod.* 178 (2018) 618–643, <https://doi.org/10.1016/j.jclepro.2017.11.207>.
- [4] Z. Guo, A. Tu, C. Chen, D.E. Lehman, Mechanical properties, durability, and life-cycle assessment of concrete building blocks incorporating recycled concrete aggregates, *J. Clean. Prod.* 199 (2018) 136–149, <https://doi.org/10.1016/j.jclepro.2018.07.069>.
- [5] W. Li, J. Xiao, C. Shi, C.S. Poon, Structural behaviour of composite members with recycled aggregate concrete – An overview, *Adv. Struct. Eng.* 18 (2015) 919–938, <https://doi.org/10.1260/1369-4332.18.6.919>.
- [6] X. He, Z. Zheng, M. Ma, Y. Su, J. Yang, H. Tan, Y. Wang, B. Strnadl, New treatment technology: The use of wet-milling concrete slurry waste to substitute cement, *J. Clean. Prod.* 242 (2020), 118347, <https://doi.org/10.1016/j.jclepro.2019.118347>.
- [7] N. Makul, Cost-benefit analysis of the production of ready-mixed high-performance concrete made with recycled concrete aggregate: A case study in Thailand, *Heliyon* 6 (2020) e04135.
- [8] A. Juan-Valdés, D. Rodríguez-Robles, J. García-González, M.I. Sánchez de Rojas Gómez, M. Ignacio Guerra-Romero, N. De Belie, J.M. Morán-del Pozo, Mechanical and microstructural properties of recycled concretes mixed with ceramic recycled cement and secondary recycled aggregates. A viable option for future concrete, *Constr. Build. Mater.* 270 (2021), <https://doi.org/10.1016/j.conbuildmat.2020.121455>.
- [9] P. Jagadesh, A. Juan-Valdés, M.I. Guerra-Romero, J.M. Morán-Del Pozo, J. García-González, R. Martínez-García, Effect of design parameters on compressive and split tensile strength of self-compacting concrete with recycled aggregate: An overview, *Appl. Sci.* 11 (2021) 6028, <https://doi.org/10.3390/app11136028>.
- [10] J. Pacheco, J. de Brito, C. Chastre, L. Evangelista, Experimental investigation on the variability of the main mechanical properties of concrete produced with coarse recycled concrete aggregates, *Constr. Build. Mater.* 201 (2019) 110–120, <https://doi.org/10.1016/j.conbuildmat.2018.12.200>.
- [11] M. Etxeberria, E. Vázquez, A. Marí, M. Barra, Influence of amount of recycled coarse aggregates and production process on properties of recycled aggregate concrete, *Cem. Concr. Res.* 37 (2007) 735–742, <https://doi.org/10.1016/j.cemconres.2007.02.002>.
- [12] F. López-Gayarre, P. Serna, A. Domingo-Cabo, M.A. Serrano-López, C. López-Colina, Influence of recycled aggregate quality and proportioning criteria on recycled concrete properties, *Waste Manag.* 29 (2009) 3022–3028, <https://doi.org/10.1016/j.wasman.2009.07.010>.
- [13] H. Zhang, Y. Zhao, Performance of recycled aggregate concrete in a real project, *Adv. Struct. Eng.* 17 (2014) 895–906, <https://doi.org/10.1260/1369-4332.17.6.895>.
- [14] H. Mefteh, O. Kebaili, H. Oucief, L. Berredjem, N. Arabi, Influence of moisture conditioning of recycled aggregates on the properties of fresh and hardened concrete, *J. Clean. Prod.* 54 (2013) 282–288, <https://doi.org/10.1016/j.jclepro.2013.05.009>.
- [15] Z.J. Grdic, G.A. Toplicic-Curcic, I.M. Despotovic, N.S. Ristic, Properties of self-compacting concrete prepared with coarse recycled concrete aggregate, *Constr. Build. Mater.* 24 (2010) 1129–1133, <https://doi.org/10.1016/j.conbuildmat.2009.12.029>.
- [16] D. Shanmugavel, T. Selvaraj, R. Ramadoss, S. Raneri, Interaction of a viscous biopolymer from cactus extract with cement paste to produce sustainable concrete, *Constr. Build. Mater.* 257 (2020), 119585, <https://doi.org/10.1016/j.conbuildmat.2020.119585>.
- [17] G. Mamo, B. Mattiasson, Alkaliphiles: the emerging biological tools enhancing concrete durability, *Alkaliphiles Biotechnol.* 172 (2020) 293–342, <https://doi.org/10.1007/10.2019.94>.
- [18] D. Losic, J.G. Mitchell, N.H. Voelcker, Diatomaceous lessons in nanotechnology and advanced materials, *Adv. Mater.* 21 (2009) 2947–2958, <https://doi.org/10.1002/adma.200803778>.
- [19] M. Terracciano, L. De Stefano, I. Rea, Diatoms green nanotechnology for biosilica-based drug delivery systems, *Pharmaceutics* 10 (2018) 1–15, <https://doi.org/10.3390/pharmaceutics10040242>.
- [20] M. Georges, A. Bourguiba, M. Boutouil, D. Chateigner, O. Jolly, P. Claquin, Interaction between the diatom *Cylindrotheca closterium* and a siliceous mortar in a silica-limited environment, *Constr. Build. Mater.* 321 (2022), 126277, <https://doi.org/10.1016/j.conbuildmat.2021.126277>.
- [21] A.C. Anil, J.S. Patil, S. Mitbavkar, S.D. Silva, S. Hegde, R. Naik, Role of diatoms in marine biofouling, *Recent Adv. Appl. Asp. Indian Mar. Algae with Ref. to Glob. Scenar.* 1 (2006) 351–365. <http://drs.nio.org/drs/handle/2264/810>.
- [22] P.J. Molino, R. Wetherbee, The biology of biofouling diatoms and their role in the development of microbial slimes, *Biofouling* 24 (2008) 365–379, <https://doi.org/10.1080/08927010802254583>.
- [23] F. Sullivan, T. Novel materials for mitigation of diatom biofouling on marine sensors, *Instrument. ViewPoint* 11 (2011) 39.
- [24] W. Fu, A. Chaiboonchoe, B. Dohai, M. Sultana, K. Baffour, A. Alzhami, J. Weston, D. Al Khairy, S. Daakour, A. Jaiswal, D.R. Nelson, A. Mystikou, S. Brynjólfsson, K. Salehi-Ashtiani, GPCR genes as activators of surface colonization pathways in a model marine diatom, *IScience* 23 (2020), 101424, <https://doi.org/10.1016/j.isci.2020.101424>.
- [25] W. De Muynck, D. Debrouwer, N. De Belie, W. Verstraete, Bacterial carbonate precipitation improves the durability of cementitious materials, *Cem. Concr. Res.* 38 (2008) 1005–1014, <https://doi.org/10.1016/j.cemconres.2008.03.005>.

- [26] W.-S. Ng, M.-L. Lee, S.-L. Hii, An Overview of the Factors Affecting Microbial-Induced Calcite Precipitation and its Potential Application in Soil Improvement, *Int. J. Civ. Environ. Eng.* 6 (2012) 188–194, <https://pdfs.semanticscholar.org/dc1f/0ed47ecdc6b4a1ce6b46ab6a4114ae60503.pdf>.
- [27] J. Xu, X. Wang, W. Yao, Coupled effects of carbonation and bio-deposition in concrete surface treatment, *Cem. Concr. Compos.* 104 (2019), 103358, <https://doi.org/10.1016/j.cemconcomp.2019.103358>.
- [28] M.A. Yazdi, E. Gruyaert, K. Van Tittelboom, N. Boon, N. De Belie, Treatment with nano-silica and bacteria to restore the reduced bond strength between concrete and repair mortar caused by aggressive removal techniques, *Cem. Concr. Compos.* 120 (2021), 104064, <https://doi.org/10.1016/j.cemconcomp.2021.104064>.
- [29] R.B. Ardalan, N. Jamshidi, H. Arabameri, A. Joshaghani, M. Mehrnejad, P. Sharafi, Enhancing the permeability and abrasion resistance of concrete using colloidal nano-SiO<sub>2</sub> oxide and spraying nanosilicon practices, *Constr. Build. Mater.* 146 (2017) 128–135, <https://doi.org/10.1016/j.conbuildmat.2017.04.078>.
- [30] Y. Geng, S. Li, D. Hou, X. Chen, Z. Jin, Effect of SiO<sub>2</sub> sol/silane emulsion in reducing water and chloride ion penetration in concrete, *Coatings* 10 (2020), <https://doi.org/10.3390/coatings10070682>.
- [31] H. Li, Y. Shi, High-strength, waterproof, corrosion-resistant nano-silica carbon nanotube cementitious composites, *Materials (Basel)* 13 (2020), <https://doi.org/10.3390/MA13173737>.
- [32] M.R. Sakr, M.T. Bassuoni, A. Ghazy, Durability of concrete superficially treated with nano-silica and silane/ nano-clay coatings, *Transp. Res. Rec.* 2675 (2021) 21–31, <https://doi.org/10.1177/0361198120953160>.
- [33] E. Axtell III, G. Sakoske, D. Swiler, M. Hensel, M. Baumann, D. Matalka, G. Nuccetelli, Structured Self-Cleaning Surfaces and Method of Forming Same, US 2006/0246277, 2006.
- [34] EN 197-1. Cement. Part 1: Composition, specifications and conformity criteria for common cements; AENOR: Madrid, Spain, 2011.
- [35] EN 933-1. Tests for geometrical properties of aggregates. Part 1: Determination of particle size distribution. Sieving method; AENOR: Madrid, Spain, 2012.
- [36] EN 1097-6. Tests for mechanical and physical properties of aggregates. Part 6: Determination of particle density and water absorption; AENOR: Madrid, Spain, 2014.
- [37] Structural Code; Royal Decree 470/2021, Spanish Ministry of the Presidency, Relations with the Courts and Democratic Memory; AENOR: Madrid, Spain, 2021.
- [38] EN 12620:2003+A1. Aggregates for concrete; AENOR: Madrid, Spain, 2009.
- [39] A. Djerbi Tegger, Determining the water absorption of recycled aggregates utilizing hydrostatic weighing approach, *Constr. Build. Mater.* 27 (2012) 112–116, <https://doi.org/10.1016/j.conbuildmat.2011.08.018>.
- [40] EN 933-11. Tests for geometrical properties of aggregates. Part 11: Classification test for the constituents of coarse recycled aggregate; AENOR: Madrid, Spain, 2009.
- [41] EN 12390-3 Testing hardened concrete. Part 3: Compressive strength of test specimens; AENOR: Madrid, Spain, 2020.
- [42] W. Admiraal, Influence of light and temperature on the growth rate of estuarine benthic diatoms in culture, *Mar. Biol.* 39 (1976) 1–9, <https://doi.org/10.1007/BF00395586>.
- [43] S. Lacoursière, I. Lavoie, M.A. Rodríguez, S. Campeau, Modeling the response time of diatom assemblages to simulated water quality improvement and degradation in running waters, *Can. J. Fish. Aquat. Sci.* 68 (2011) 487–497, <https://doi.org/10.1139/F10-162>.
- [44] EN 13946. Water quality. Guidance for the routine sampling and preparation of benthic diatoms from rivers and lakes; AENOR: Madrid, Spain, 2014.
- [45] EN 14407. Water quality. Guidance for the identification and enumeration of benthic diatom samples from rivers and lakes; AENOR: Madrid, Spain, 2015.
- [46] G. Hofmann, M. Werum, H. Lange-Bertalot, Diatomeen im Süßwasser-Benthos von Mitteleuropa : Bestimmungsflora Kieselalgen für die ökologische Praxis ; über 700 der häufigsten Arten und ihre Ökologie, 2011.
- [47] C. Lecointe, M. Coste, J. Prygiel, "Omnia": software for taxonomy, calculation of diatom indices and inventories management, *Hydrobiologia* 269 (1993) 509–513.
- [48] ISO 10260. Measurement of biochemical parameters. Spectrometric determination of the chlorophyll a concentration, London, United Kingdom, 1992.
- [49] UNE 83966. Concrete durability. Test methods. Conditioning of concrete test pieces for the purpose of gas permeability and capillary suction tests; AENOR: Madrid, Spain, 2008.
- [50] UNE 83982. Concrete durability. Test methods. Determination of the capillary suction in hardened concrete. Fagerlund method; AENOR: Madrid, Spain, 2008.
- [51] EN 12390-8. Testing hardened concrete. Part 8: Depth of penetration of water under pressure; AENOR: Madrid, Spain, 2020.
- [52] EN 12390-6. Testing hardened concrete. Part 6: Tensile splitting strength of test specimens; AENOR: Madrid, Spain, 2010.
- [53] ImageJ. Computer Software, Version 1.8.0; National Institutes of Health, Bethesda, MD, USA. Available online: <https://imagej.nih.gov/ij/> (accessed on 2022).
- [54] F. Stazi, A. Nacci, F. Tittarelli, E. Pasqualini, P. Munafò, An experimental study on earth plasters for earthen building protection: The effects of different admixtures and surface treatments, *J. Cult. Herit.* 17 (2016) 27–41, <https://doi.org/10.1016/j.culher.2015.07.009>.
- [55] EN 16302. Conservation of cultural heritage. Test methods. Measurement of water absorption by pipe method; AENOR: Madrid, Spain, 2016.
- [56] J. Lu, K. Wang, M.L. Qu, Experimental determination on the capillary water absorption coefficient of porous building materials: A comparison between the intermittent and continuous absorption tests, *J. Build. Eng.* 28 (2020), 101091, <https://doi.org/10.1016/j.job.2019.101091>.
- [57] J.J. Howland, A.R. Martín, Estudio de la absorción capilar y la sorptividad de hormigones con áridos calizos cubanos, *Mater. Constr.* 63 (2013) 515–527, <https://doi.org/10.3989/mc.2013.04812>.
- [58] EN 1504-2. Products and systems for the protection and repair of concrete structures. Definitions, requirements, quality control and evaluation of conformity. Part 2: Surface protection systems for concrete; AENOR: Madrid, Spain, 2005.
- [59] J. Zhang, S. Hong, B. Dong, L. Tang, C. Lin, Z. Liu, F. Xing, Water distribution modelling of capillary absorption in cementitious materials, *Constr. Build. Mater.* 216 (2019) 468–475, <https://doi.org/10.1016/j.conbuildmat.2019.05.023>.
- [60] J. Liu, F. Xing, B. Dong, H. Ma, D. Pan, Study on water sorptivity of the surface layer of concrete, *Mater. Struct. Constr.* 47 (2014) 1941–1951, <https://doi.org/10.1617/s11527-013-0162-x>.
- [61] A.A. Shirzadi Javid, P. Ghoddousi, M. Zareechian, A. Habibnejad Korayem, Effects of spraying various nanoparticles at early ages on improving surface characteristics of concrete pavements, *Int. J. Civ. Eng.* 17 (2019) 1455–1468, <https://doi.org/10.1007/s40999-019-00407-4>.
- [62] P. Matar, J. Barhoun, Effects of waterproofing admixture on the compressive strength and permeability of recycled aggregate concrete, *J. Build. Eng.* 32 (2020), 101521, <https://doi.org/10.1016/j.job.2020.101521>.
- [63] P.G. Quedou, E. Wirquin, C. Bokhoree, A sustainable approach in using construction and demolition waste materials in concrete, *World J. Eng.* 18 (2021) 826–840, <https://doi.org/10.1108/WJE-05-2020-0161>.
- [64] J.H. Yoo, H.S. Lee, M.A. Ismail, An analytical study on the water penetration and diffusion into concrete under water pressure, *Constr. Build. Mater.* 25 (2011) 99–108, <https://doi.org/10.1016/j.conbuildmat.2010.06.052>.
- [65] S. Liu, R. Wang, J. Yu, X. Peng, Y. Cai, B. Tu, Effectiveness of the anti-erosion of an MICP coating on the surfaces of ancient clay roof tiles, *Constr. Build. Mater.* 243 (2020), 118202, <https://doi.org/10.1016/j.conbuildmat.2020.118202>.
- [66] A. Chiovitti, T.M. Dugdale, R. Wetherbee, Diatom adhesives: molecular and mechanical properties, *Biol. Adhes.* 1 (2006) 79–103, [https://doi.org/10.1007/978-3-540-31049-5\\_5](https://doi.org/10.1007/978-3-540-31049-5_5).